



2022 DRAGON 5 SYMPOSIUM
MID-TERM RESULTS REPORTING
17-21 OCTOBER 2022



PROJECT ID. 59197
UTILIZING SINO-EUROPEAN EARTH
OBSERVATION DATA TOWARDS AGRO-
ECOSYSTEM HEALTH DIAGNOSIS AND
SUSTAINABLE AGRICULTURE



MONDAY, 17/OCTOBER/2022

ID. 59197

PROJECT TITLE: UTILIZING SINO-EUROPEAN EARTH OBSERVATION DATA TOWARDS AGRO-ECOSYSTEM HEALTH DIAGNOSIS AND SUSTAINABLE AGRICULTURE

PRINCIPAL INVESTIGATORS: LIANG LIANG, CARSTEN MONTZKA

CO-AUTHORS: SHUGUO WANG, BAGHER BAYAT, WENSONG LIU, SHIRIN MORADI, RAHUL RAJ, DAVID MENGEN, LU XU, JORDAN BATES, YUQUAN QU, RENMIN YANG, WENQIN HUANG, VISAKH SIVAPRASAD

PRESENTED BY: CARSTEN MONTZKA





David Megen



Carsten Montzka



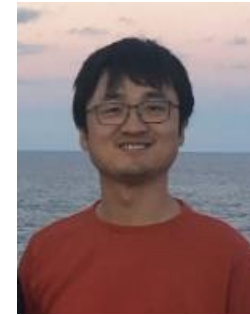
Bagher Bayat



Jordan Bates



Wensong Liu



Renmin Yang



Liang Liang



Shuguo Wang



Yuquan Qu



Rahul Raj



Wenqin Huang



Shirin Moradi



Qianjie Wang



Jin Shi



Siyi Qiu



Yanyan Shi

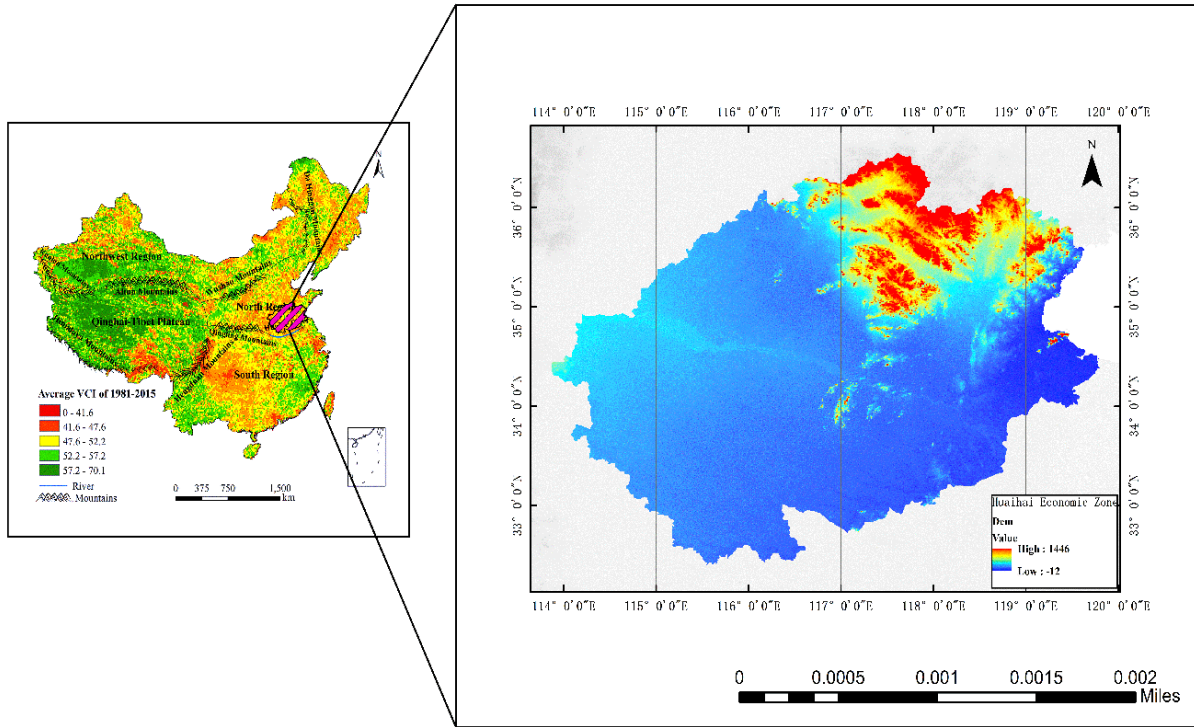


Visakh Sivaprasad

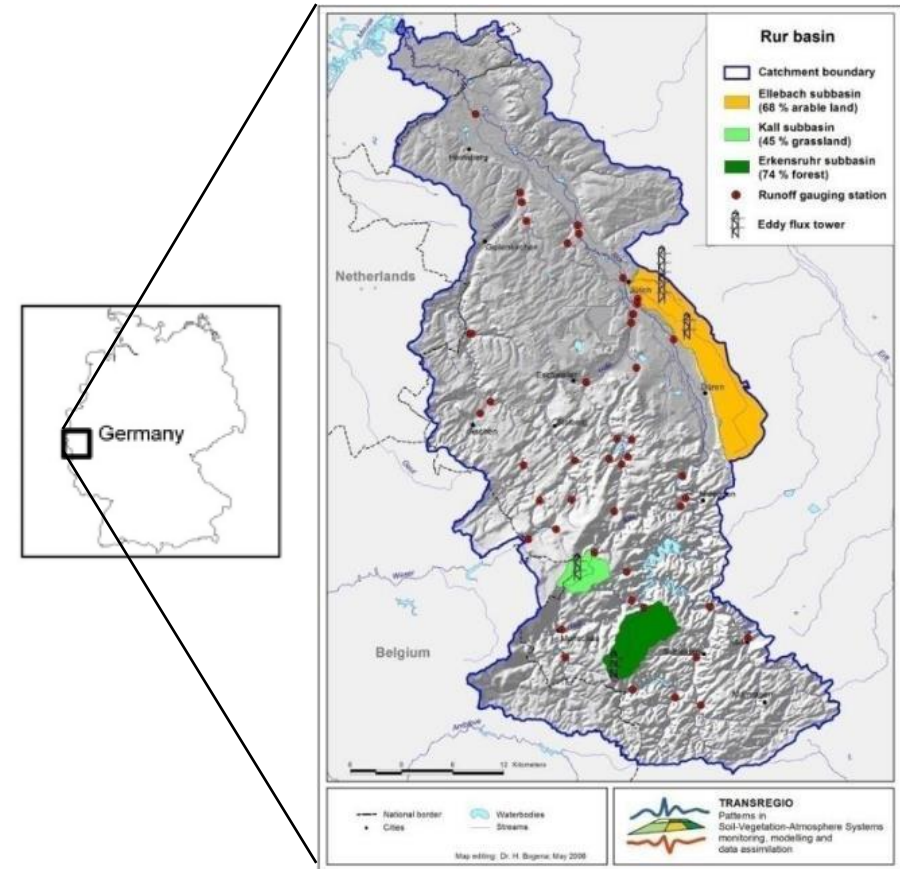
Central aims:

- to monitor essential variables in agriculture based on various in situ and remote observations
- to investigate agricultural processes and to carry out a full agro-ecosystem health diagnosis by data assimilation
- to conserve, protect, and improve the efficiency of the use of natural resources to facilitate sustainable agricultural development
- to prepare for agricultural applications of future missions like ROSE-L, CHIME, CIMR, and LSTM.





The Huaihai Economic Zone, China



The Rur Catchment, Germany

Carbon farming as ecosystem service

“Agriculture is the ONE sector that has the ability to transform from a net emitter of CO₂ to a net sequesterer of CO₂ —there is no other human managed realm with this potential”.

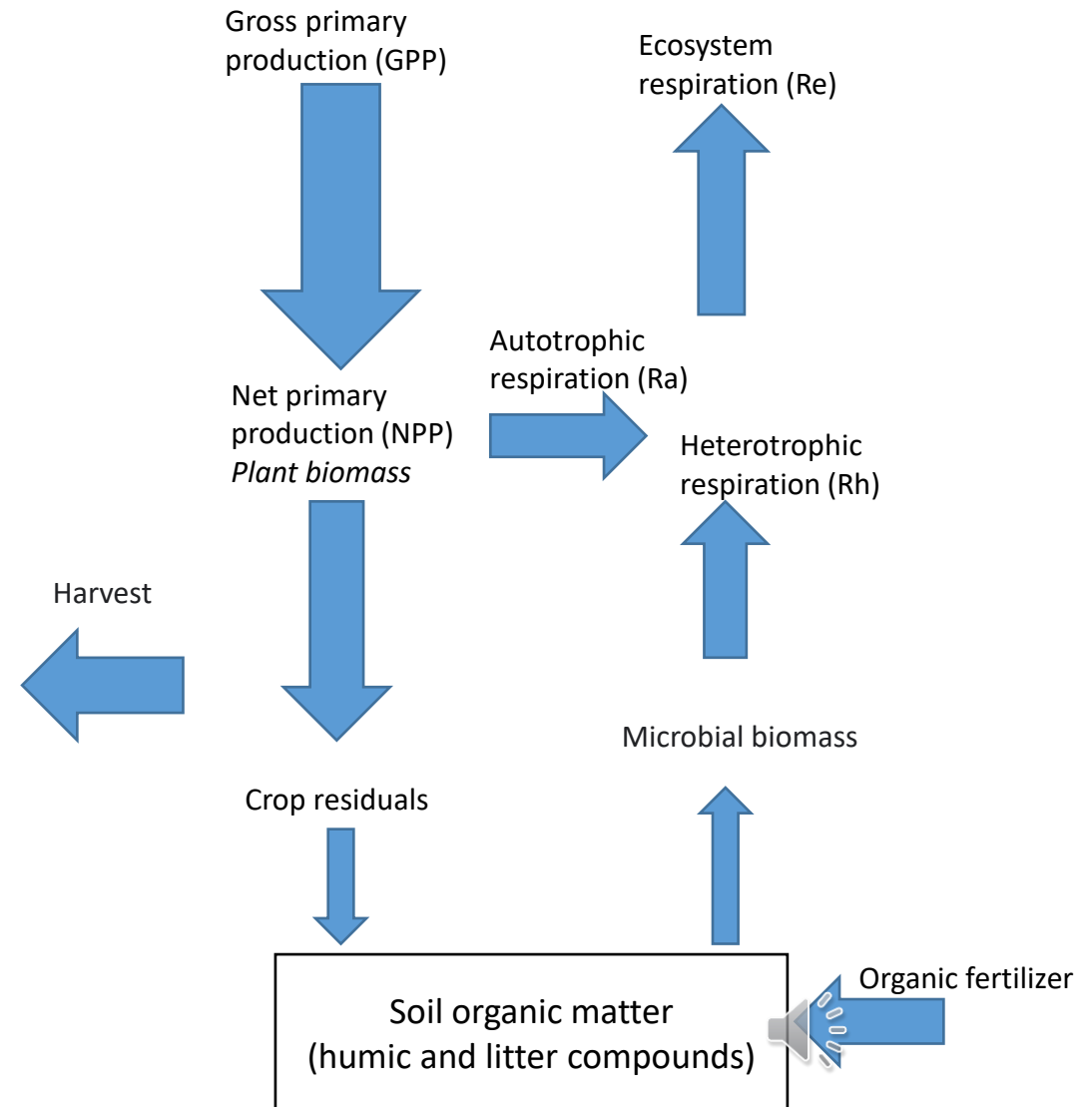
Contribution of agroecosystem:

- 10–14% of global anthropogenic greenhouse gas emissions
- store soil carbon up to 1 GT year⁻¹, offset around 10% of the annual GHG emissions of 8–10 GT year⁻¹

Carbon budget for crops:

- Net ecosystem carbon budget (NECB) = net ecosystem production (NEP) + carbon gain (e.g., due to organic fertiliser, seeds, root vegetables) + carbon loss in the biomass at harvest or during fire.

=> **Multivariate agricultural monitoring**



Towards agroecosystem carbon budget monitoring several intermediate steps are necessary:

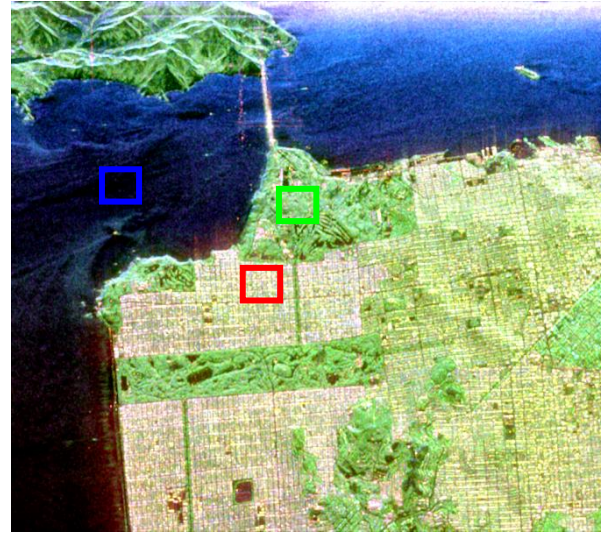
1. Crop identification by SAR polarimetry
2. LAI estimation by a hybrid inversion strategy
3. Soil moisture estimation by C-band SAR
4. Agricultural water stress monitoring by MSG-SEVIRI
5. Monitoring drought evolution based on vegetation indices
6. Monitoring Net Primary Productivity (NPP)
7. Estimation of vegetation carbon sinks (NEP)

Presented in the following (each topic 2 slides)

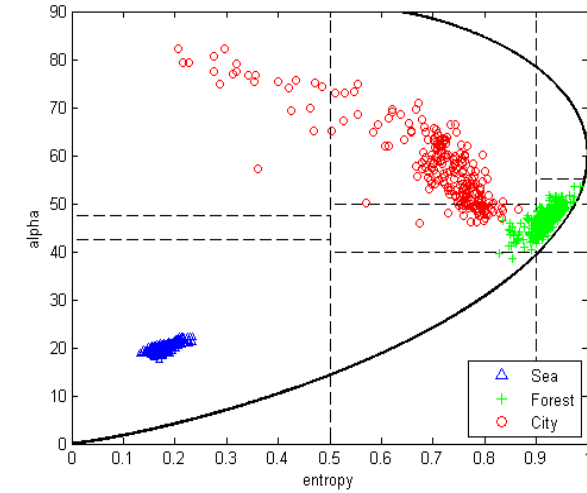




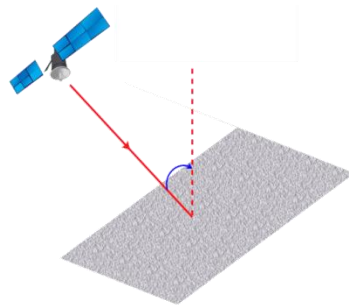
(a) Intensity image



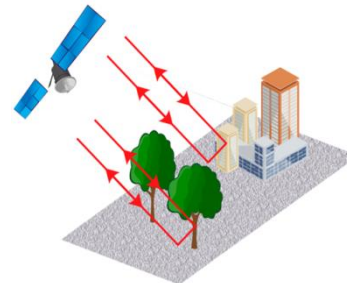
(b) PauliRGB Pseudocolor image



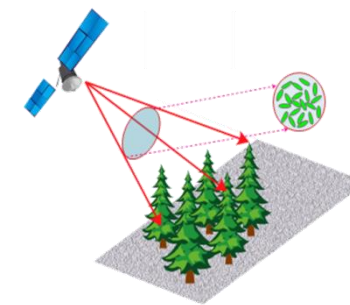
(c) H/ α plane



Odd-bounce scattering

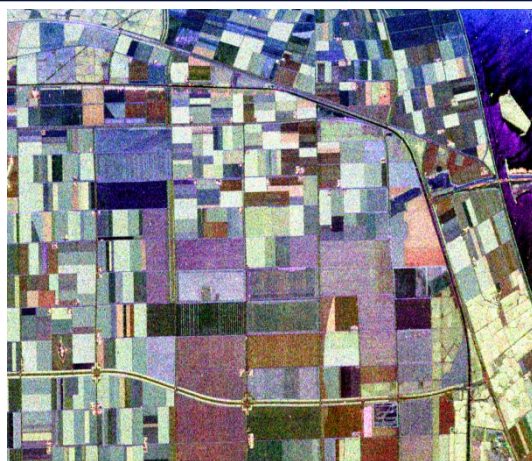


Double-bounce scatter



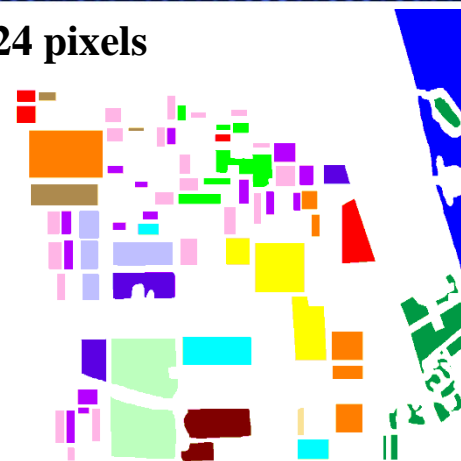
Volume scatter





Flevoland (AIRSAR,1989)

750 × 1024 pixels



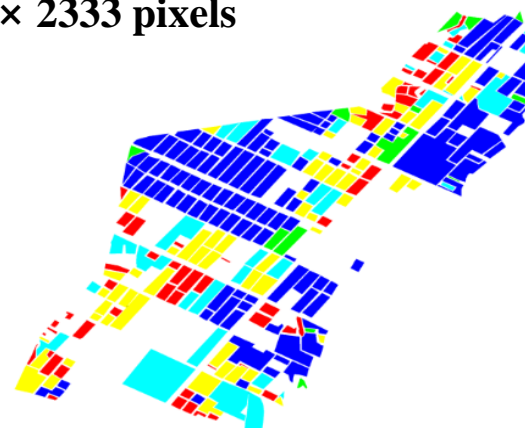
Classification results (Flevoland)

- | | |
|----|-----|
| 油菜 | 小麦A |
| 林地 | 小麦B |
| 豌豆 | 小麦C |
| 大麦 | 建筑物 |
| 裸土 | 水体 |
| 苜蓿 | 豇豆 |
| 甜菜 | 马铃薯 |
| 草地 | |



Lingshui County, Hainan (CETC38, 2012)

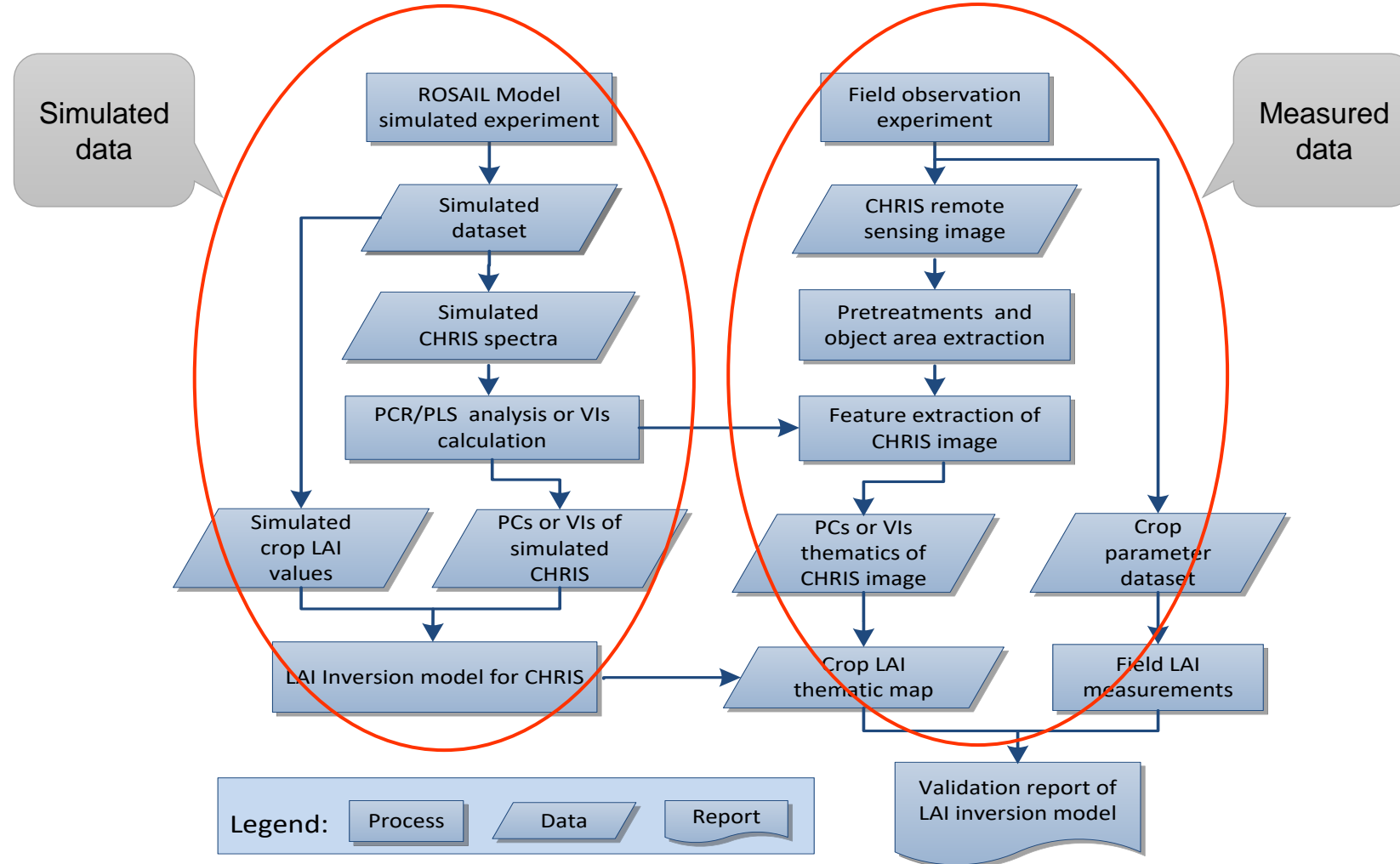
2220 × 2333 pixels



Classification results (Lingshui County)

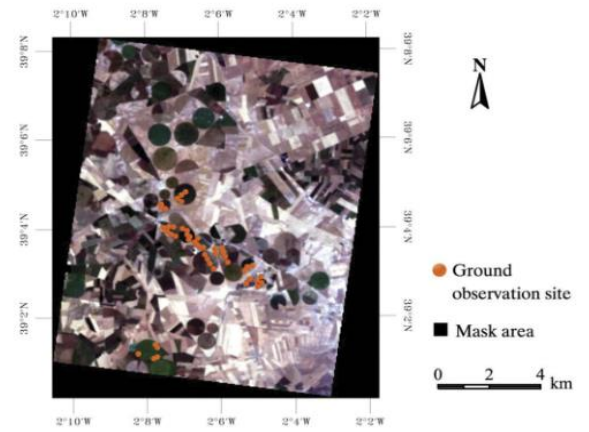
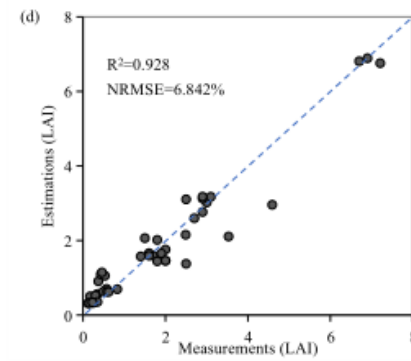
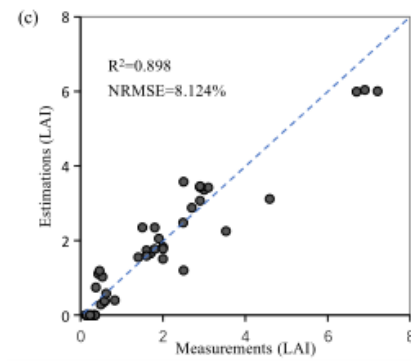
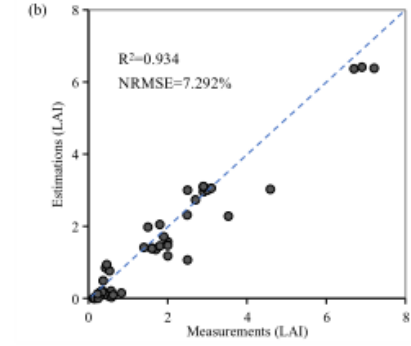
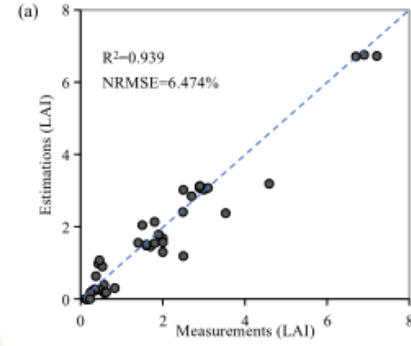
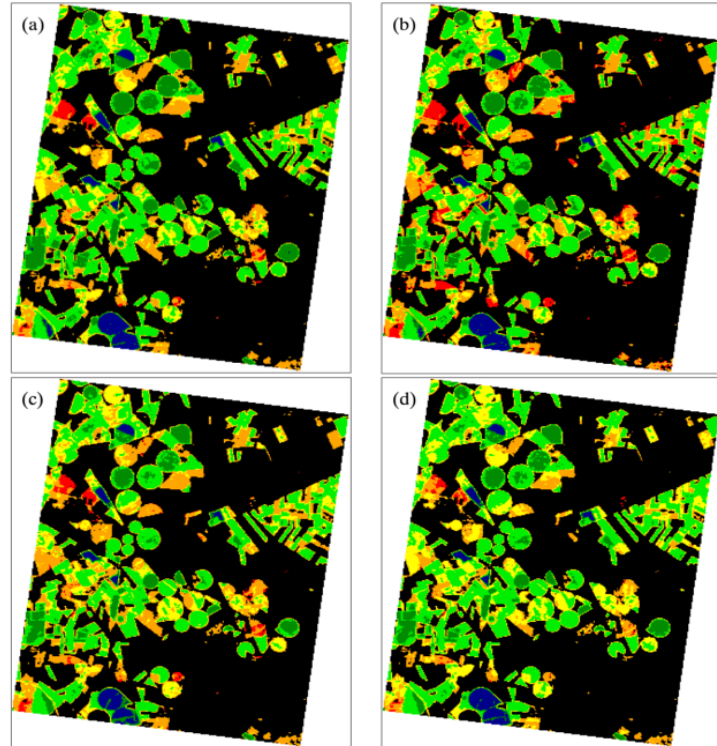
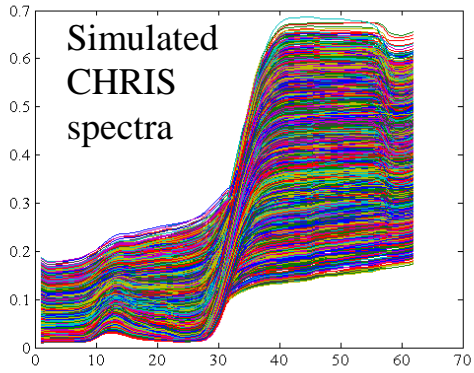
- | | |
|--|------|
| | 分蘖期 |
| | 拔节期 |
| | 穗分化期 |
| | 开花期 |
| | 成熟期 |





Flow chart of vegetation LAI remote sensing estimation based on integrated inversion strategy





CHRIS image of study area

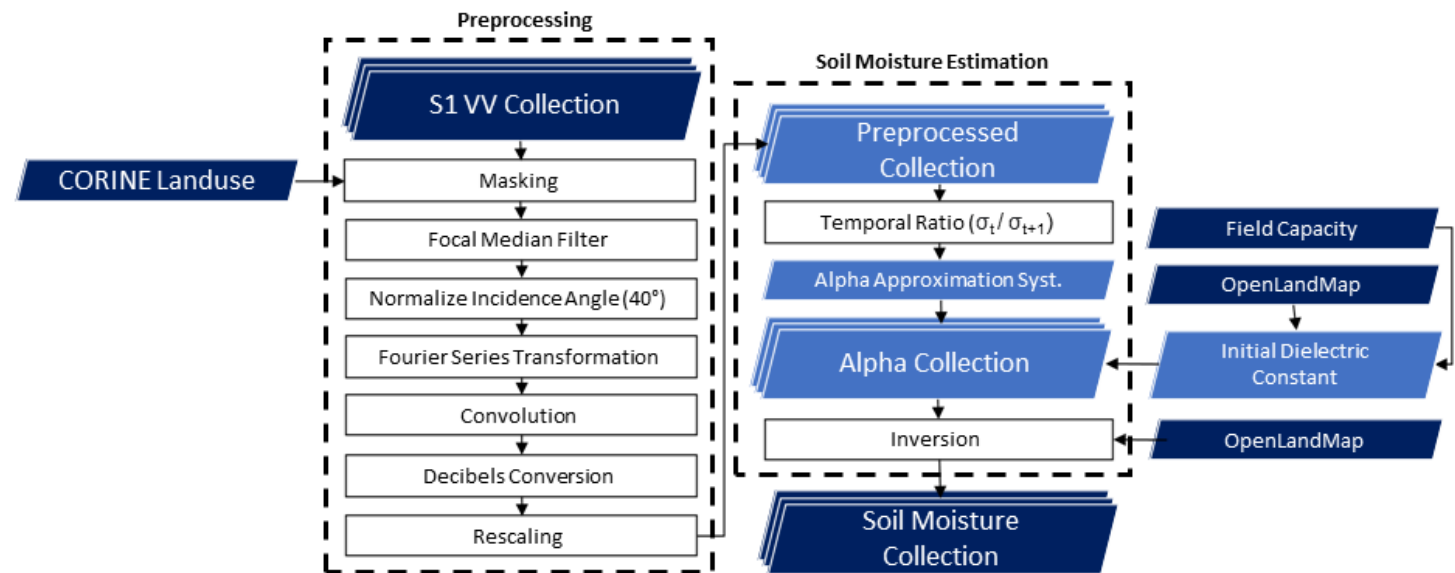
Spatial distribution map of the crop LAI predicted from the CHRIS remote sensing image and various RFR models in Sentinel-3 Experiment: (a) Specific2_PLS_RFR, (b) Specific1_PLS_RFR, (c) Generic_PLS_RFR, (d) Specific2_OSAVI_RFR.

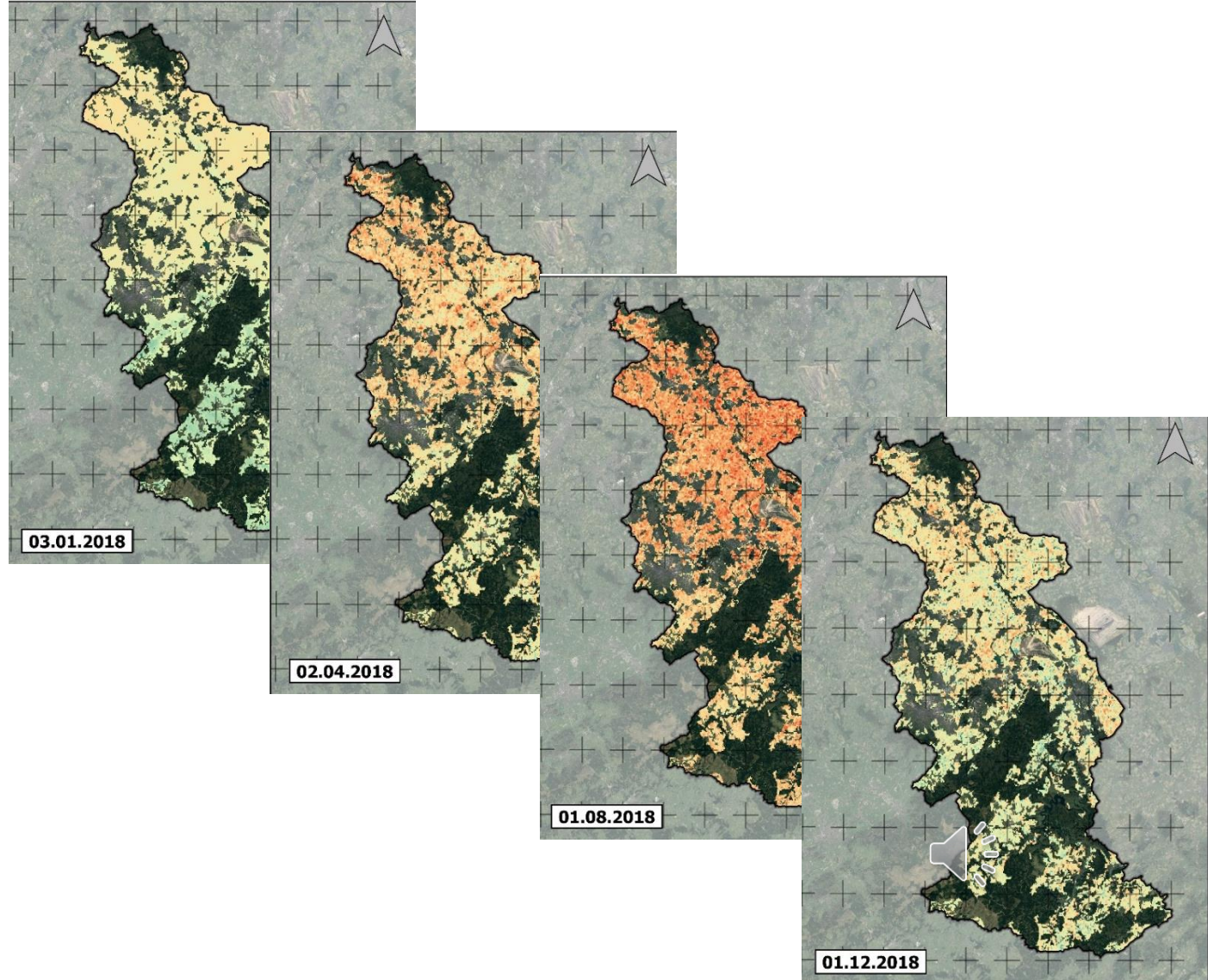
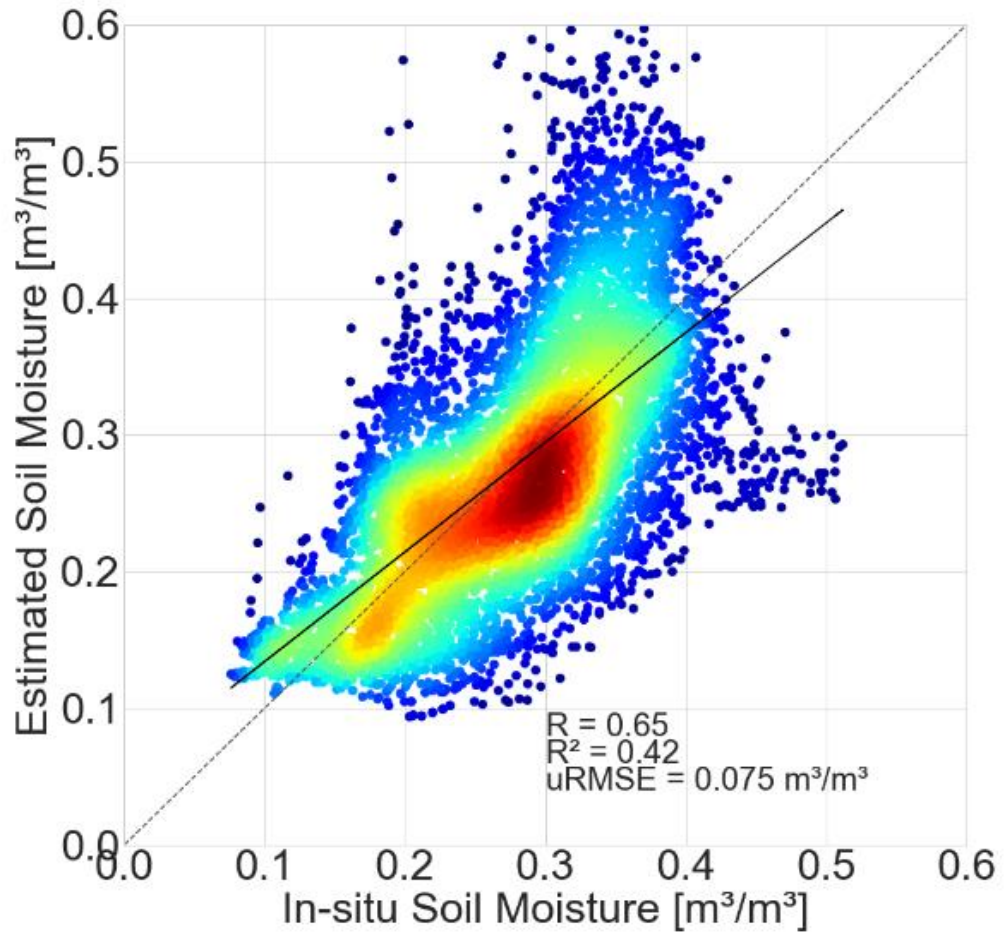
Ground-measured LAI versus the LAI estimated from the RFR inversion model in the Sentinel-3 Experiment: (a) Specific2_PLS_RFR, (b) Specific1_PLS_RFR, (c) Generic_PLS_RFR, and (d) Specific2_OSAVI_RFR.

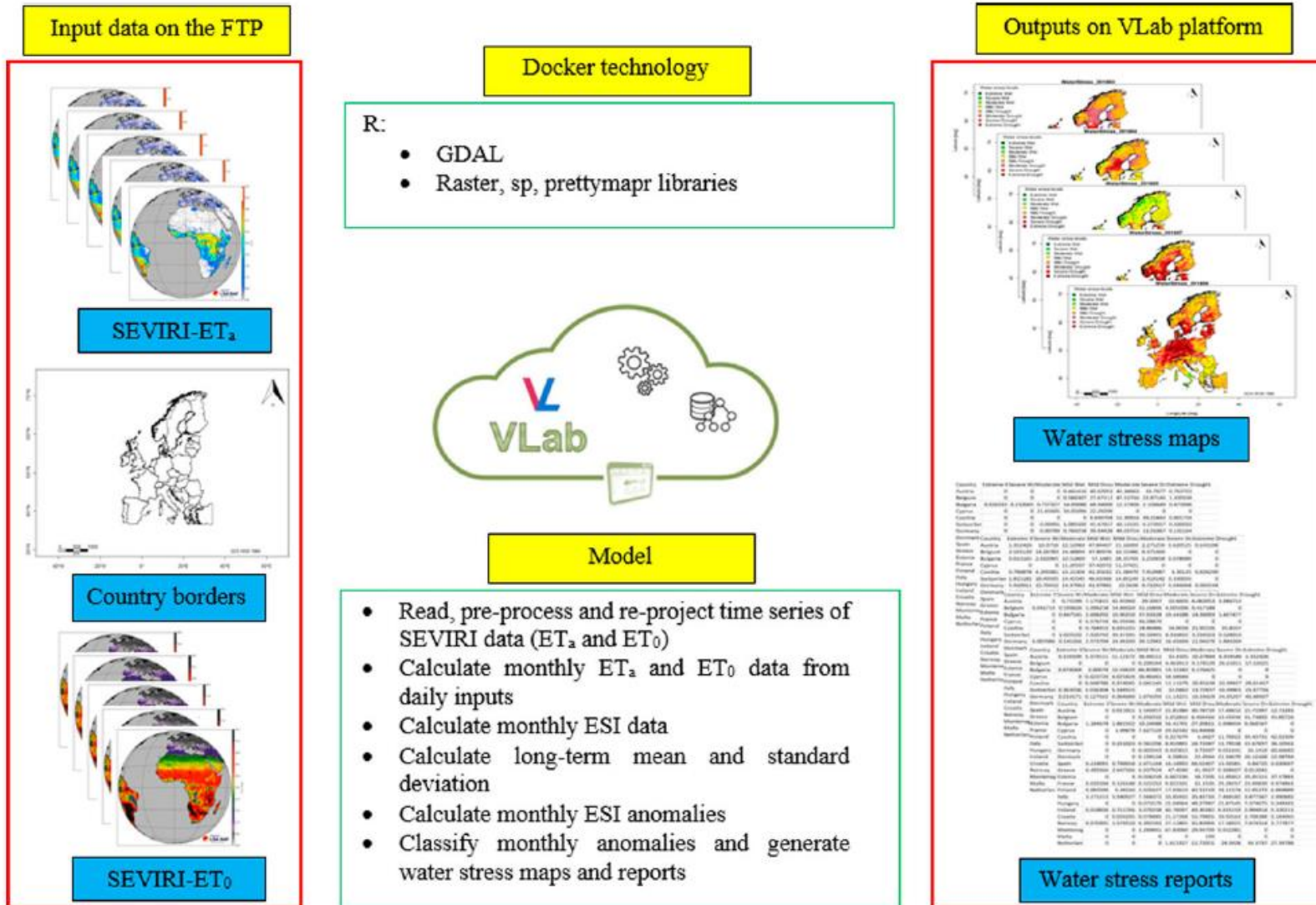
Basic principle: Between two consecutive SAR observations, change in backscattering signal is caused by a change in dielectric constant and incidence angle, as other surface parameters do not change considerably within these short time interval

Workflow can be divided into two sections:

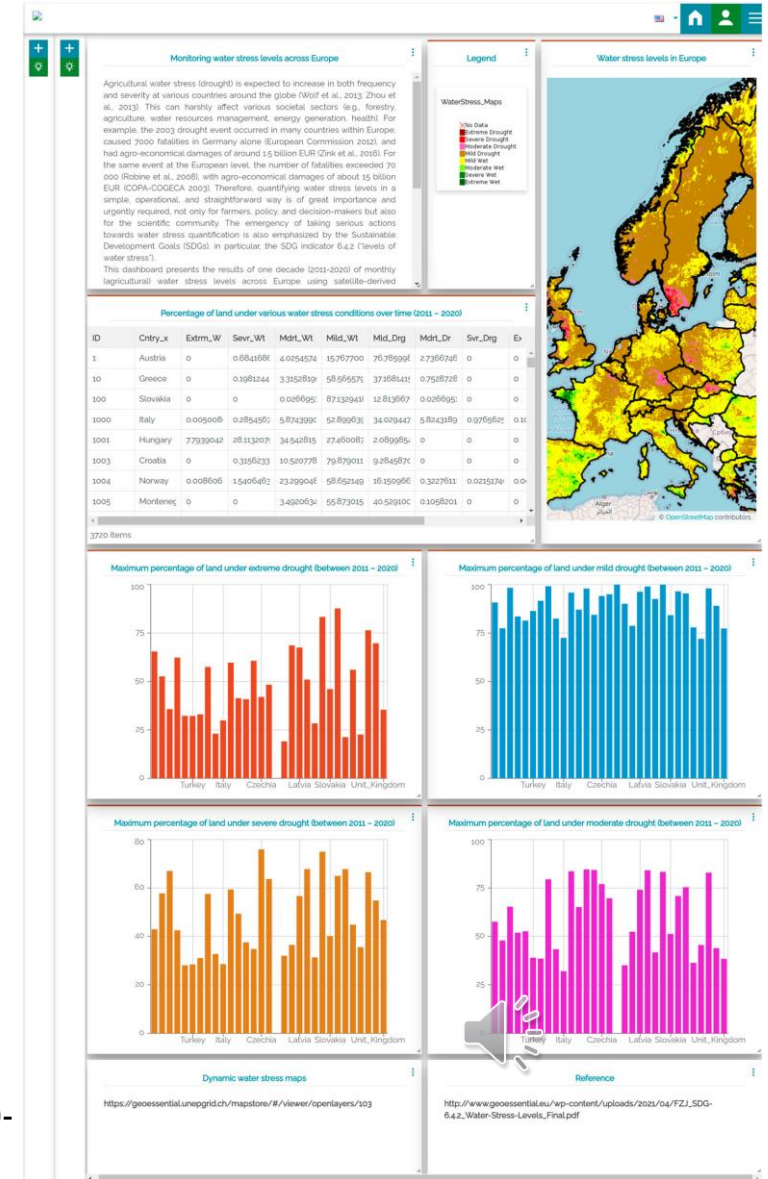
- Pre-processing of Sentinel-1 SAR
- Soil moisture estimation







- Daily time series of actual and potential evapotranspiration by SEVIRI
- Reports for policy information and decision support
- Monthly agricultural water stress maps for Europe
- Processed in VLAB on AWS, stored in GeoServer, documented in GeoNetwork, and made available through MapStore



Bagher Bayat, Carsten Montzka, Alexander Graf, Gregory Giuliani, Mattia Santoro & Harry Vereecken (2022) One decade (2011–2020) of European agricultural water stress monitoring by MSG-SEVIRI: workflow implementation on the Virtual Earth Laboratory (VLab) platform, International Journal of Digital Earth, 15:1, 730-747, DOI:10.1080/17538947.2022.2061617

Analysis of drought occurrence frequency and change trend in China using long time series VCI, TVDI index products and meteorological data

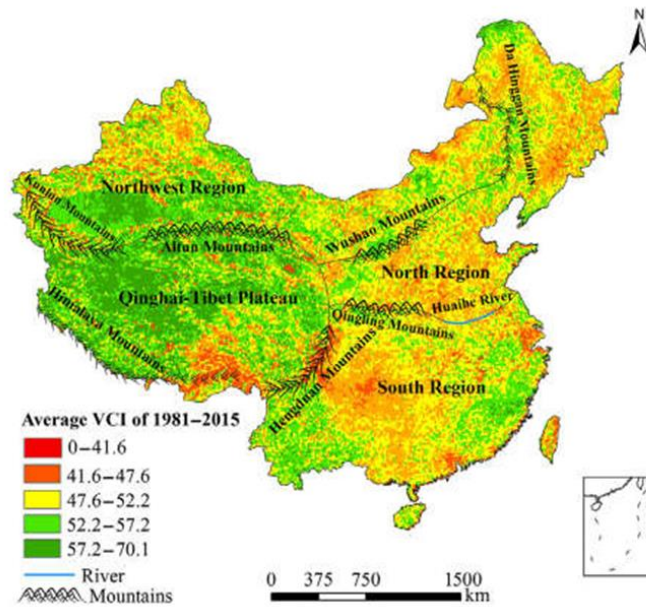


Fig. 1. Overview of the study area. The background is the average vegetation condition index (VCI) value from 1981 to 2015.

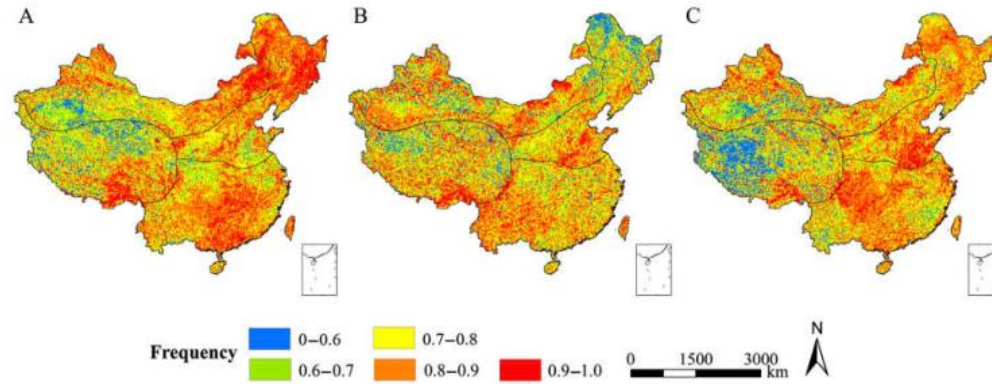


Fig. 2. Spatial distribution of the total drought occurrence frequencies in China for (A) spring, (B) summer, and (C) autumn.

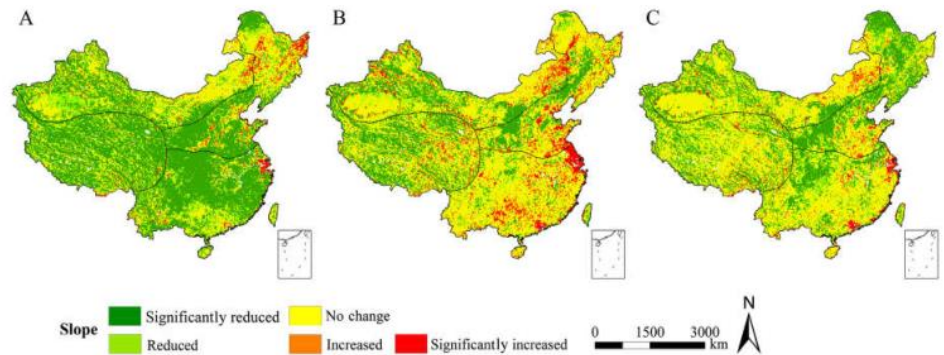
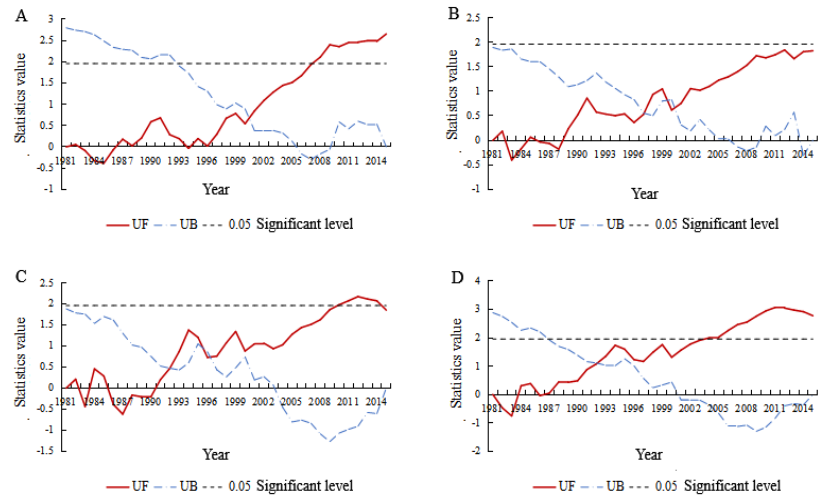


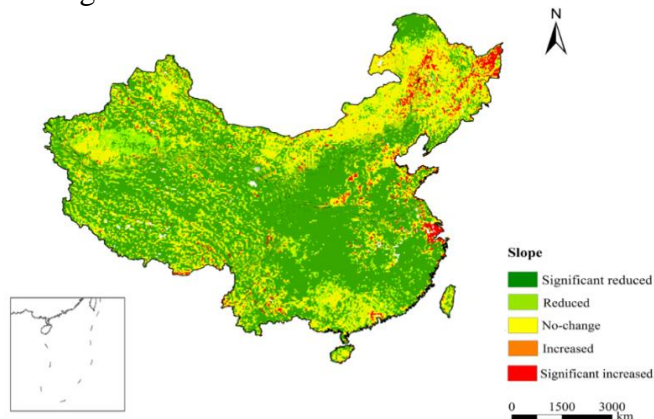
Fig. 4. Vegetation condition index trends from 1981 to 2015 in China for the (A) spring, (B) summer, and (C) autumn.

激活
 转码

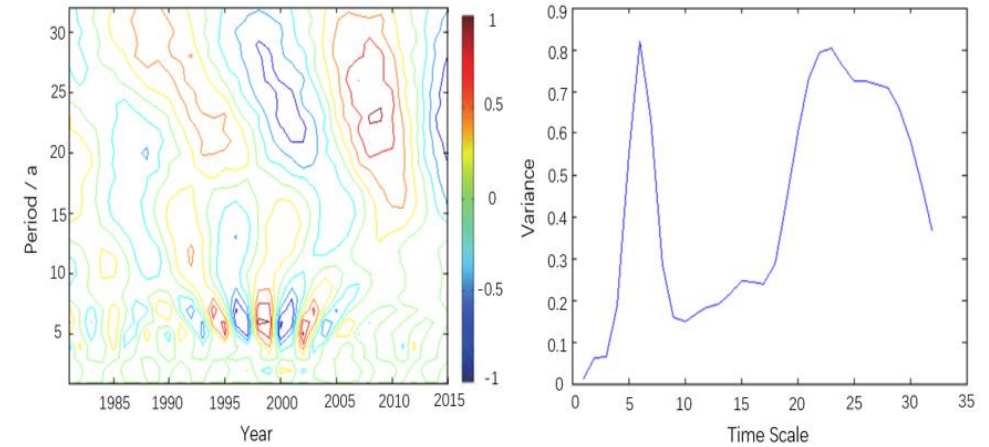




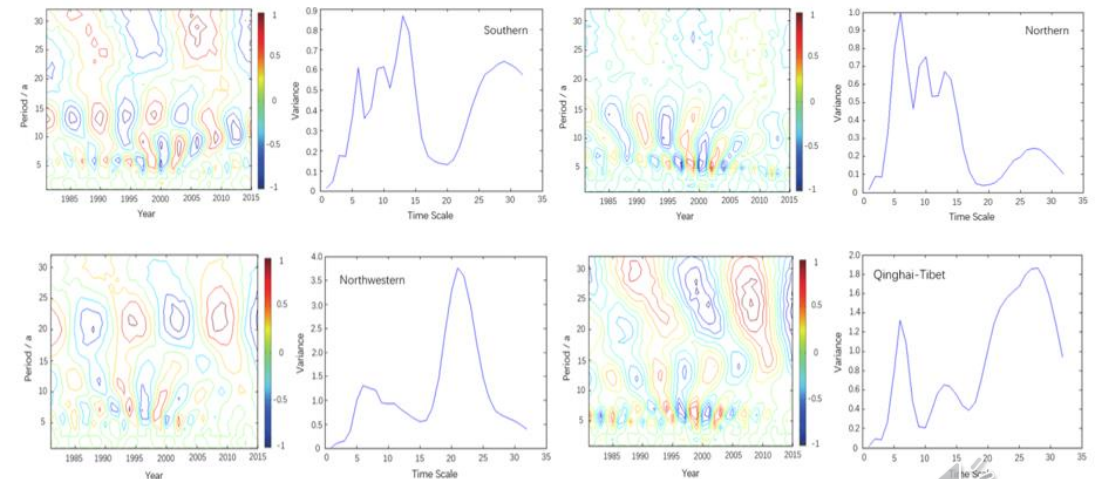
Mann-Kendall mutation analysis results of VCI time series for various regions of China



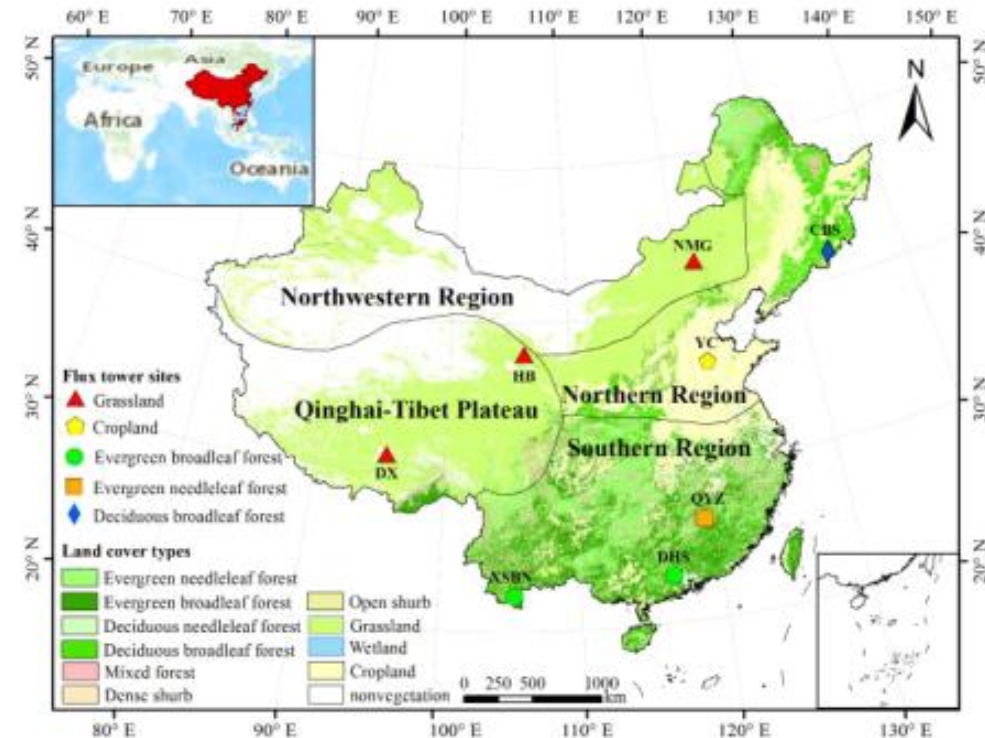
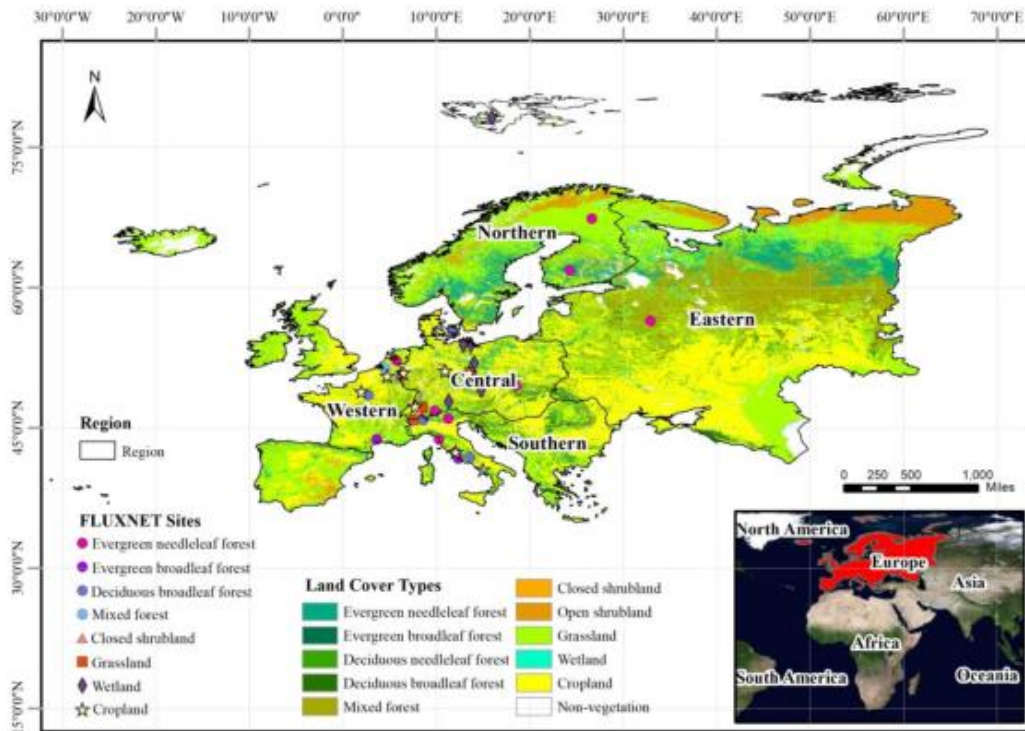
Slope trend of the average VCI in spring from 1981-2015 in China



Wavelet time series analysis of spring VCI in China, 1981-2015.



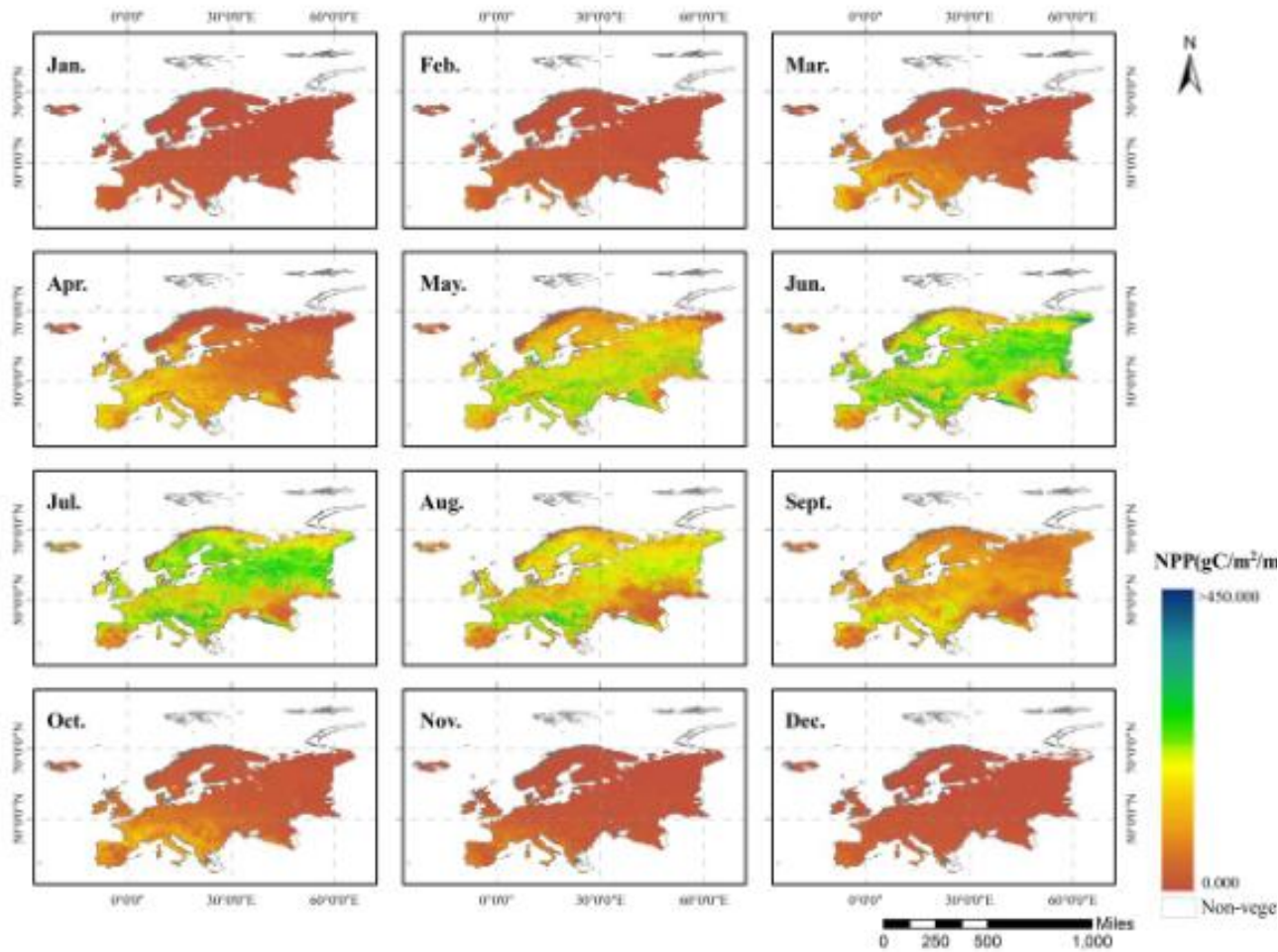
Spring VCI wavelet time series analysis maps for the southern (A), northern (B), northwestern (C) and Qinghai-Tibet (D) regions of China.



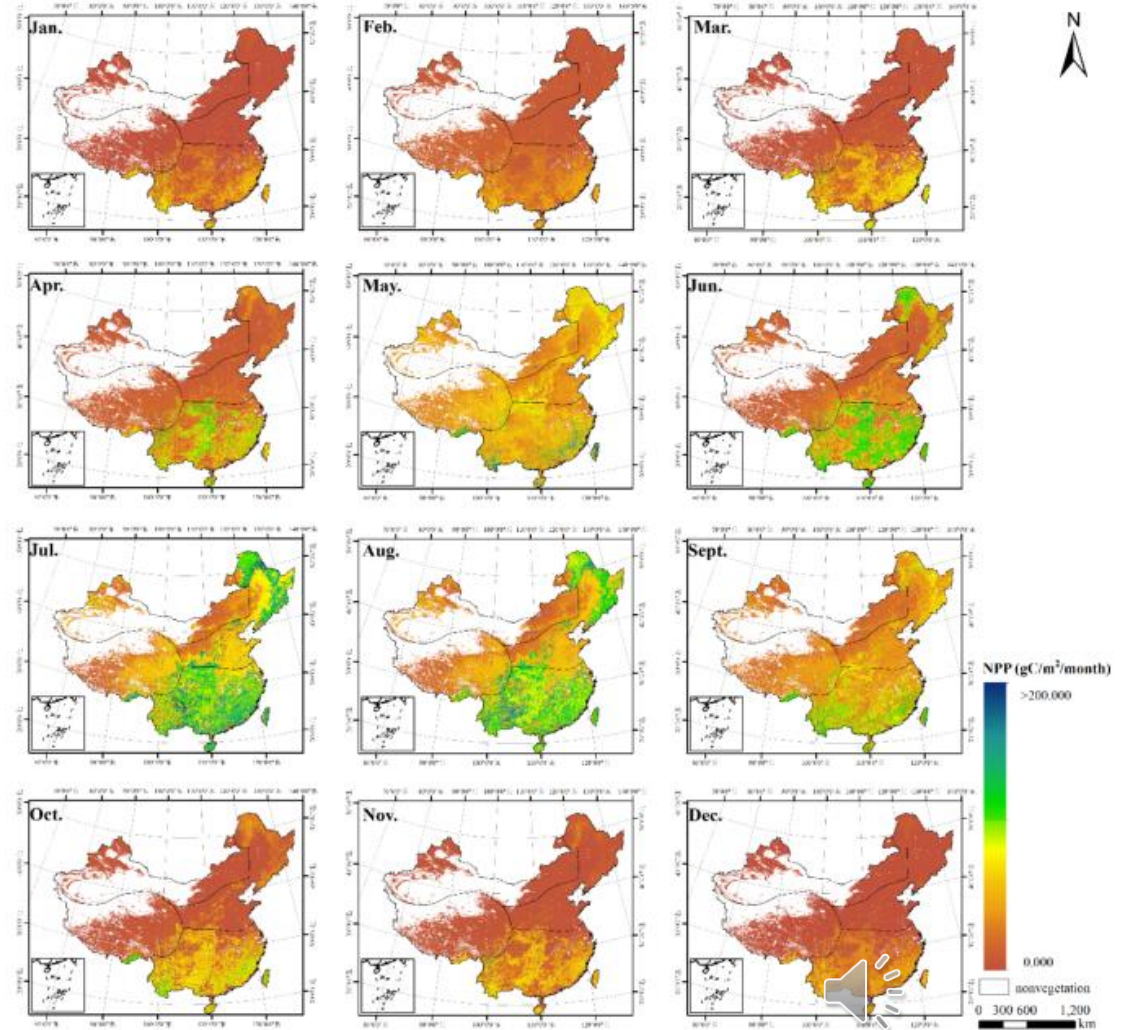
Types of Land Cover and Distribution of Flux Stations of Study Area

Land cover types, the locations of the eight flux tower sites and the distribution of the four geographical regions.

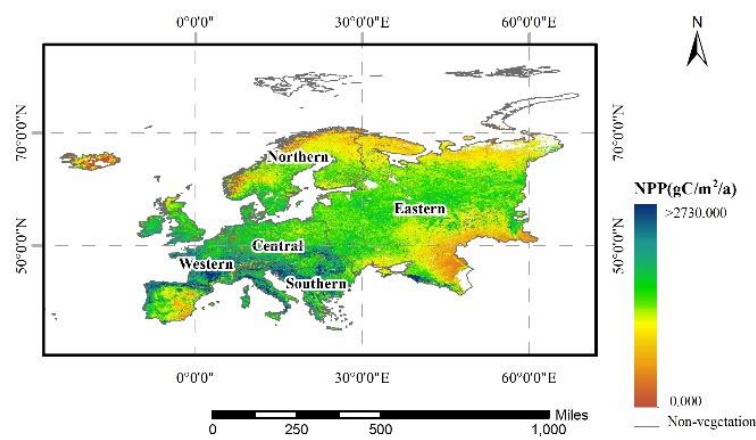




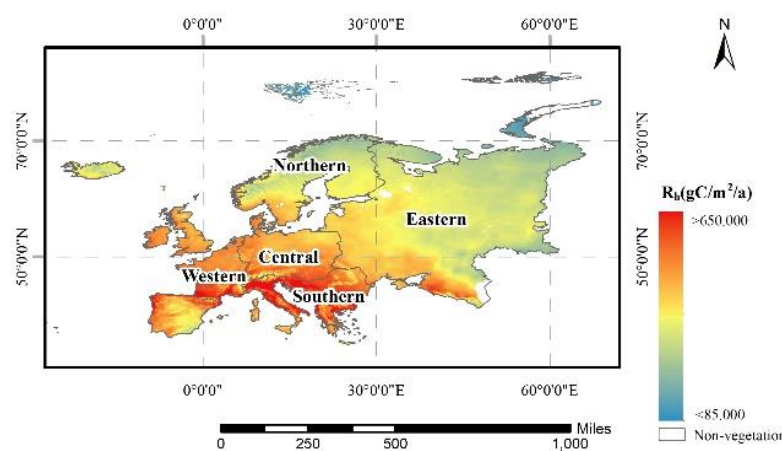
Spatiotemporal distribution of Monthly NPP in Europe Based on Optimized Model.



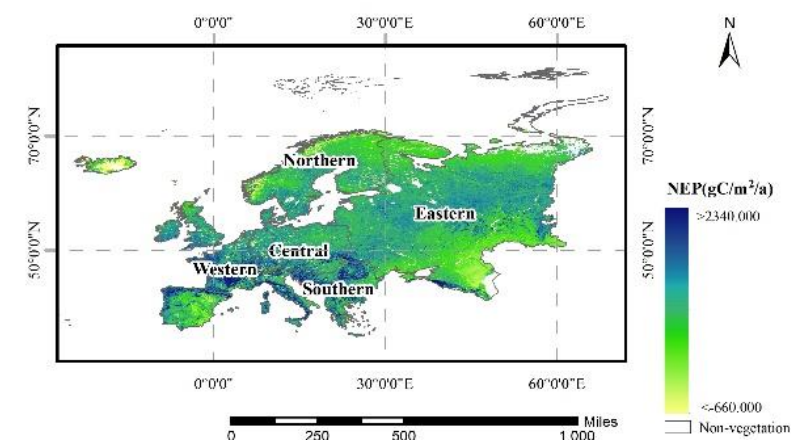
Spatial pattern of monthly NPP estimated over China by the improved CASA model.



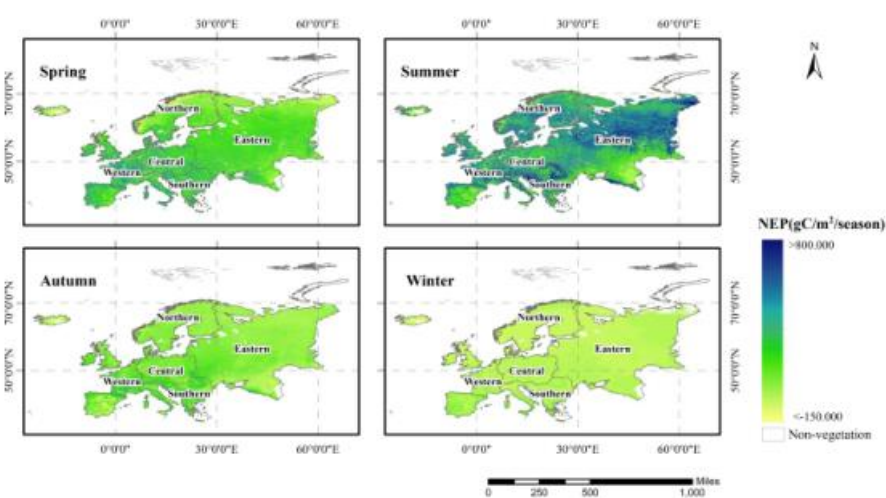
Annual NPP of Europe



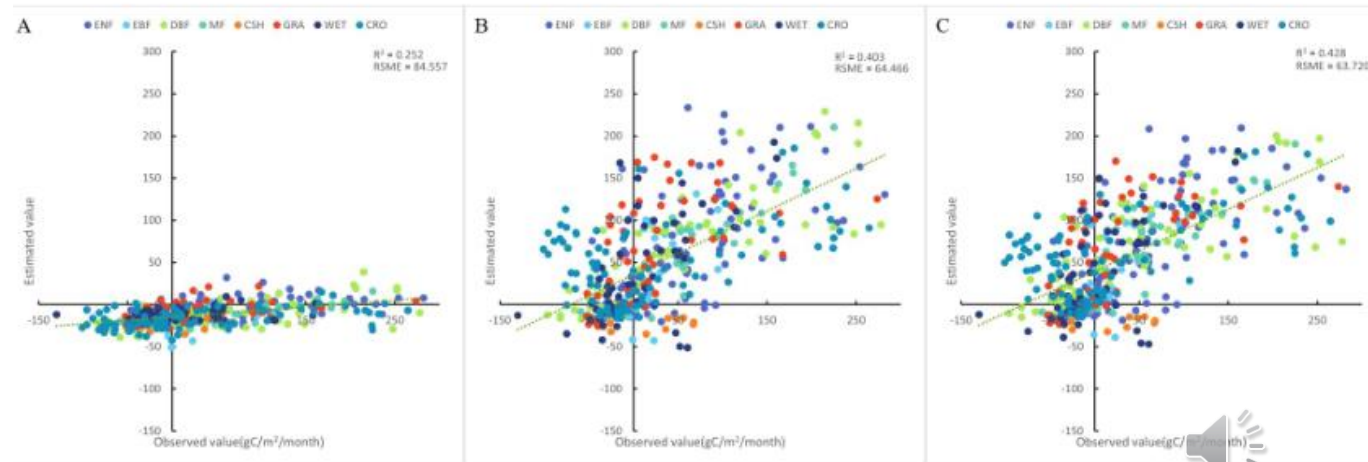
Annual Rh of Europe



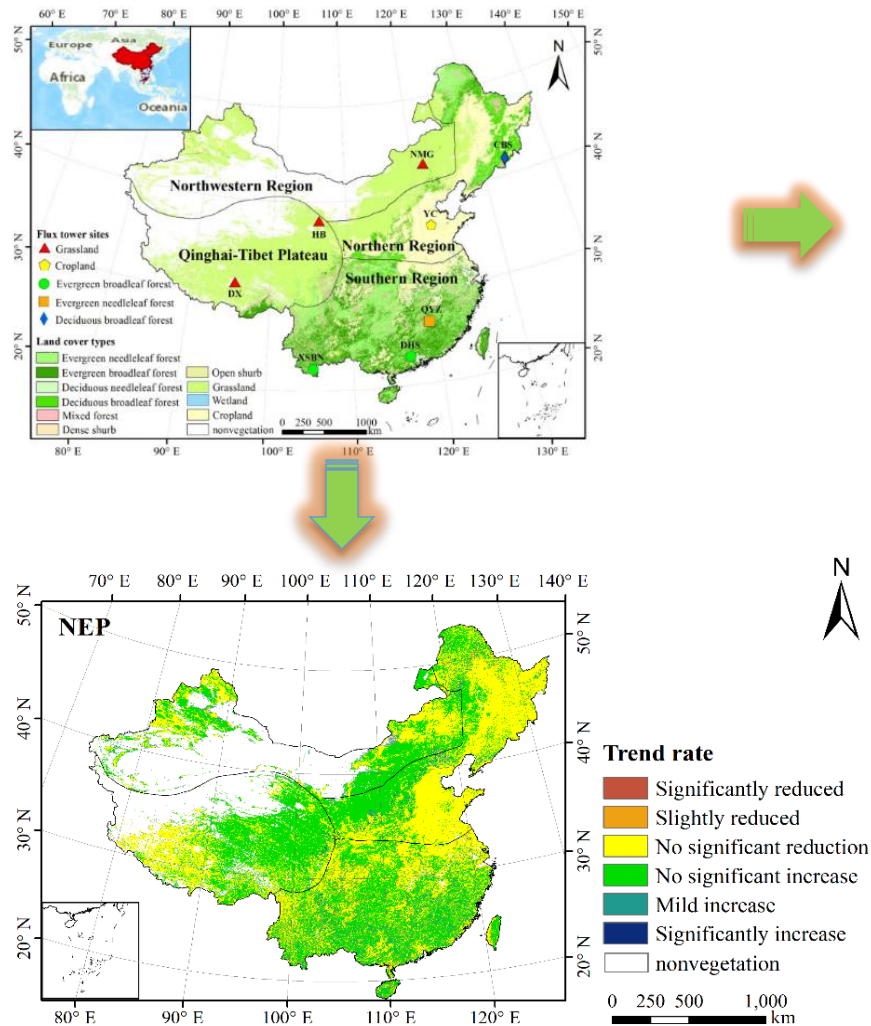
Annual NEP of Europe



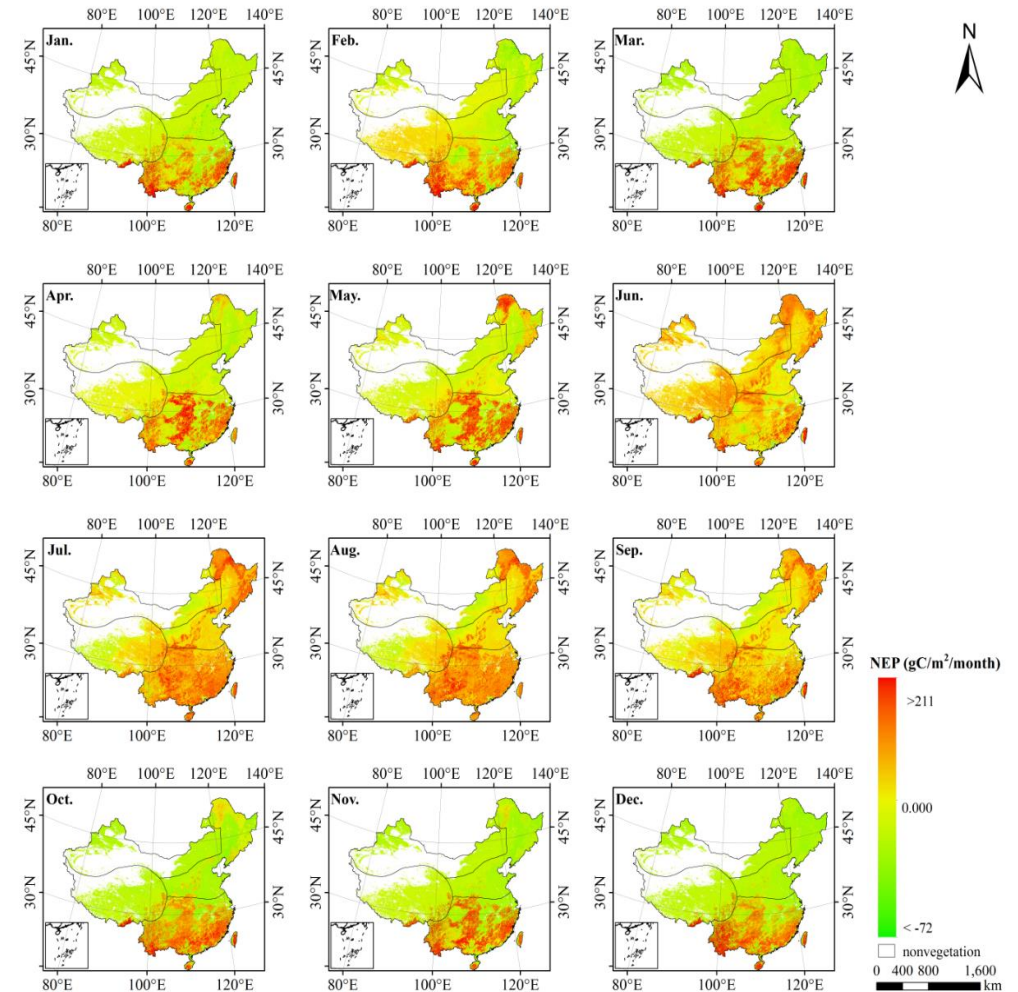
Spatiotemporal Distribution of Seasonal NEP in Europe during 2014.



Comparison of NEP Observations and Estimates. (A. Verifications results of original model; B. Verification results with optimized ϵ_{max} ; C. Verification results with optimized ϵ_{max} and T_{opt})



Spatial distribution of summer NEP trends in China from 2001 to 2016



Monthly average estimation results of NEP of terrestrial ecosystem vegetation in China





Name	Institution	Poster title	Contribution
David Mengen	Research Center Jülich	Soil Moisture Remote Sensing using Sentinel-1 time series	Estimating soil moisture by the alpha approximation approach for multiple incidence angles in the Google Earth Engine





Name	Institution	Poster title	Contribution
Siyi Qiu	Jiangsu Normal University	Remote Sensing Estimation of NEP in Europe and Improvement of CASA Model	The Carnegie Ames Stanford approach (CASA) model was optimized by the maximum light use efficiency and the optimal temperature, and the NEP value of the European terrestrial ecosystem was estimated by coupling the soil respiration model.
Yanyan Shi	Jiangsu Normal University	Assessment of Classification Accuracy of Four Global Land Cover Data in Nine Urban Agglomerations	A conference paper has been published, and various ground object sample points have been collected by visual interpretation on Google Earth.
Jin Shi	Jiangsu Normal University	A remote sensing extraction method for garlic distribution in PiZhou City Using GEE cloud platform	To obtain accuracy of classification by obtaining characteristic information of garlic. Through this, we can improve the efficiency of garlic extraction by remote sensing.
Qianjie Wang	Jiangsu Normal University	Insights into Spatiotemporal Variations of Net Primary Productivity of Terrestrial Vegetation in Africa During 1981-2018	Data products such as spatial and temporal distribution patterns and dynamic changes of global NPP can be obtained to determine the main factors affecting global NPP.



Thank you!



Dr. Liang Liang (梁亮)

School of geography, geomatics and planning

Jiangsu Normal University, Xuzhou 221116, China

liang_rs@jsnu.edu.cn

Dr. Carsten Montzka

Forschungszentrum Jülich GmbH, IBG-3,
Leo-Brandt-Strasse, 52428 Jülich, Germany

c.montzka@fz-juelich.de

